

Development and Applications of Quantum Dot-based Molecularly Imprinted Polymer Composites for Optosensing of Carbofuran in Water

Qiang ZHOU,^{*,**} Chengcheng LIU,^{***} Hong ZHANG,^{*,**} Chunjie ZHAO,^{***} and Yanhong WANG^{*,**†}

^{*}*Institute of Applied Ecology, Chinese Academy of Sciences, Shenyang 110016, China*

^{**}*Ministry of Agriculture Laboratory of Risk Assessment of Environment Factors for Quality and Safety of Agro-Products, Shenyang 110016, China*

^{***}*School of Pharmacy, Shenyang Pharmaceutical University, Shenyang 110016, China*

In this paper, quantum dot (QD)-based molecularly imprinted polymer (MIP) was fabricated and successfully utilized as a fluorescent probe for highly selective and sensitive detection of carbofuran in water samples. The MIPs were synthesized followed by a multi-step swelling and polymerization method, and then labeled with CdSe/ZnS QDs *via* gradual solvent evaporation. Then the prepared QDs-MIP microspheres were introduced to flow cytometry by virtue of their good dispersibility in water, and fast adsorption and desorption. Under optimized conditions, the fluorescence intensity of QDs-MIP decreased linearly with the increasing of carbofuran in the concentration range of 1 – 20 $\mu\text{g L}^{-1}$ ($R^2 > 0.99$) and it can detect down to 0.2 $\mu\text{g L}^{-1}$ of carbofuran. This method was simple, selective and applied successfully to the optosensing of trace carbofuran in water samples with good recoveries ranging from 94.1 ± 3.7 to $98.4 \pm 4.5\%$.

Keywords Molecularly imprinted polymer, quantum dots, fluorescence quenching, carbofuran

(Received March 1, 2017; Accepted April 26, 2017; Published August 10, 2017)

Introduction

Carbofuran is a broad-spectrum insecticide, which is widely used to control insects in agriculture.¹ It is one of the most toxic carbamate pesticides and is dissolved easily in water. Its high toxicity and solubility causes accumulation in living organisms and further brings serious harm to human health and life safety.² Hence, many countries have set limit requirements of carbofuran in tap water. For example, the drinking water standards of carbofuran in the U.S., Canada and China are 5, 1.8 and 7 $\mu\text{g L}^{-1}$, respectively.^{3,4} So far, various analytical methods have been proposed to assay carbofuran and have the advantages of accuracy, sensitivity and reliability. They include gas chromatography,⁵ liquid chromatography^{6,7} and mass spectrometry.⁸ However, many disadvantages such as relatively high cost, time consuming analytical processes and the requirement of professional operators emerge simultaneously.⁹ Thus, it is of great significance to develop a simple, rapid and selective method for the optosensing of carbofuran.

Over the past decades, the molecular imprinting technique (MIT) has gained recognition as a powerful method to prepare polymeric materials with tailor-made molecular recognition binding sites.¹⁰⁻¹² The synthesis of molecular imprinting polymer (MIP) is based on the copolymerization of the template and functional monomer through the covalent/non-covalent interactions with excess cross linkers. After polymerization,

they have special cavities with corresponding steric and chemical memory with the removal of the template.¹³ Therefore, the target species can selectively rebind into MIPs through the specific interaction with these imprinted sites.¹⁴

On the other hand, quantum dots (QDs), as a kind of semiconductor nanoparticle, have attracted widespread attention.¹⁵ In recent years, QDs have been proved to be a promising type of fluorescent label due to their unique properties, including bright photoluminescence, narrow symmetric emission, broad excitation spectra, excellent photostability, good biocompatibility and large Stokes shift.¹⁶⁻¹⁸ Consequently, QDs have been widely used in diverse fields, such as pharmaceutical analysis,¹⁹ environmental pollutant detection,²⁰ and pesticide residue detection.²¹

Based on fluorescence quenching, a newly designed material that couples MIP with QDs has been explored to detect the template as a fluorescent probe.²² Zhu *et al.* introduced the core-shell CdTe quantum dot-imprinted polymers for the fluorometric determination of trace aspirin in biological samples.²³ Chen *et al.* fabricated and successfully utilized MIP-coated QDs for cyphenothrin detection in river water.²⁴ However, in these methods the value of fluorescence they collected were all by fluorescence spectrophotometry, which only supplies the fluorescence information of samples illuminated by the light source of the instrument. In addition, the polymers of each sample could not keep the same dispersion state, which resulted in inaccuracies in the detected fluorescence data. So a more effective method was needed.

As a new analytical technique, cytometric bead array (CBA) has achieved real-time and rapid detection of targeted

[†] To whom correspondence should be addressed.
E-mail: wangyh@iae.ac.cn

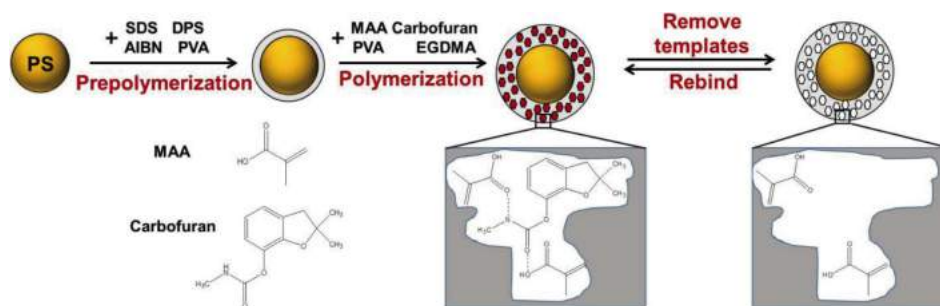


Fig. 1 The schematic illustration of the molecular imprinting process for MIP.

components in a small amount of sample.^{25,26} This CBA technique has proven superior to the traditional methods. With prominent advantages of high specificity and sensitivity, high throughput screening and easy operation, this CBA technique has been widely used to detect various components in foods, agricultural products, and environmental samples.²⁷ Furthermore, the cells and microspheres are mainly applied to the CBA technique.

In this paper, the MIPs were synthesized by a multi-step swelling to improve uniformity and sphericity. QDs-MIP composites as an optosensing material was fabricated, and a new cytometric bead assay based on fluorescence quenching method is proposed for optosensing of carbofuran in water. Fourier transform infrared spectrometer (FTIR), scanning electron microscopy (SEM), energy dispersive X-ray analysis (EDAX) and high performance liquid chromatography (HPLC) were applied to the characterization of QDs-MIP. The fluorescence quenching relationship between QDs-MIP and carbofuran was investigated while the possible quenching mechanism was discussed. Thus QDs-MIP as a fluorescence probe offers a simple, rapid and selective proposal.

Experimental

Reagents and chemicals

In brief, carbofuran and aldicarb were purchased from Huayang Chemical Reagent Co., Ltd (Shandong, China). Oil-soluble CdSe/ZnS quantum dots (Fig. S1, Supporting Information) were obtained from Wuhan Jiayuan QDs Technology Development Co., Ltd. (Wuhan, China). Ethylene glycol dimethacrylate (EGDMA) was obtained from Alfa Aesar Chemical Co. Ltd (USA). Sodium dodecyl sulfate (SDS) was purchased from Tianjin Kemiou Chemical Reagent Co., Ltd (Tianjin, China). Polyvinyl alcohol (PVA), azoisobutyronitrile (AIBN) and butyl phthalate (DBP) were obtained from Tianjin Bodi Chemical Reagent Co., Ltd (Tianjin, China). Methacrylic acid (MAA) and styrene were purchased from Tianjin Chemical Reagent Co., Ltd (Tianjin, China) and were used after vacuum distillation. All the reagents used were of at least analytical grade. High-purity water was obtained from a Milli-Q water system (Millipore, Billerica, MA, USA).

The tap water samples were collected from Shenyang City (China). All water samples were stored in a refrigerator at 4°C. The pH of tap water samples was in a range of 6.7 - 6.9.

Apparatus

The FTIR spectra of the QDs-MIP were detected with a FTIR spectrometer (Nicolet, Madison, WI, USA). Ultraviolet-visible (UV-vis) spectra were recorded by a UV spectrometer (JASCO

V-630, Japan). The morphology of the QDs-MIP was observed with a scanning electron microscope (FEI quanta 250, Netherlands). The energy dispersive X-ray analysis (EDAX, AMETEK, USA) was used to examine the elements of QDs-MIP. The adsorption performance of the MIPs and NIPs were examined by HPLC (Waters 2695, USA). The fluorescence signals were captured by flow cytometry (Cytoflex, Beckman Coulter, USA).

Preparation of QDs-MIP

Carbofuran MIPs were synthesized by a multi-step swelling and polymerization method,²⁸⁻³⁰ and then further labeled with CdSe/ZnS QDs via gradual solvent evaporation method.³¹

The synthesis method of carbofuran MIPs was as follows. At room temperature, 0.0425 g of polystyrene seed (PS) particles, 0.02 g of SDS, 0.24 mL of DBP, and 10 mL of water were added to a three-necked, round-bottomed flask with a mechanical stirrer and stirred for 15 h at 120 rpm until oil microdrops completely disappeared. After the first step swelling, 0.1642 g of AIBN (free radical initiator), 2.5 mL of toluene (porogen), 10 mL of 4.8% PVA aqueous solution and 12.5 mL of water were added. The second step swelling was carried out with stirring for 2 h at 120 rpm at room temperature. Then 0.221 g of carbofuran (template), 0.344 g of MAA (functional monomer), 2.5 mL of EGDMA (crosslinkers), 10 mL of 4.8% PVA aqueous solution and 12.5 mL of water were added. At room temperature, the third step swelling was carried out with stirring 2 h at 120 rpm. After the third-step swelling, the mixture was sealed and stirred at 50°C for 20 h at 170 rpm. The polymerization procedure was under the protection of nitrogen. The mixture was then redispersed into methanol, and the above procedure was repeated four times in methanol, twice in water and twice in tetrahydrofuran. After the polymerization, the template was removed by Soxhlet extraction with 200 mL of methanol and acetic acid (v:v = 9:1) and 250 mL of methanol until no analyte was detected. After drying in vacuum at room temperature, carbofuran imprinted polymer was obtained. The schematic illustration of the molecular imprinting process for MIPs is shown in Fig. 1. For comparison study, non-molecularly imprinted polymers (NIPs) were also synthesized without adding carbofuran and used as blank control material.

The synthesis method of QDs-MIP was carried out as follows. Under dark conditions, 40 mg of MIPs, 9 mL of chloroform and 1 mL of isopropyl alcohol were added into a 50-mL beaker and then prepared by ultrasonic dispersion for 20 min. After that, 400 µL of 525 nm CdSe/ZnS QDs was added. After ultrasonic dispersion for 10 min, the mixture was dried at 30°C under vacuum condition. Finally, the QDs-MIP was redispersed three times into ethanol. After drying at 50°C under vacuum, QDs-MIP was obtained. The QD-NIP was prepared using the same method.

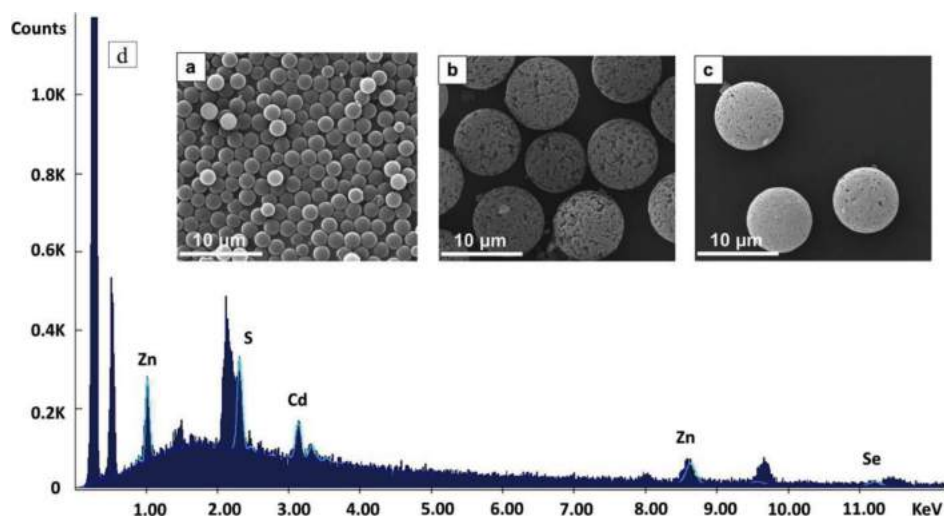


Fig. 2 SEM images of (a) PS seeds, (b) QDs-MIP and (c) QDs-NIP. (d) Energy spectrum diagram of QDs-MIP.

Adsorption capacity of QDs-MIP

To examine the adsorption performance of QDs-MIPs, a series of standard solution of carbofuran of different concentrations was prepared. First, 5.0 mg of QDs-MIPs and QDs-NIPs were mixed with 5 mL of solution containing a known concentration of either 5, 10, 20, 40, 80, 100, or 200 mg L⁻¹, respectively. After shaking for 2 h at room temperature and centrifuging at 2000 rpm for 3 min, the free concentration of carbofuran in the suspension was detected by HPLC.

Flow cytometry determination

Flow cytometry analysis was performed on Cytoflex, which was supplied by Beckman Coulter, Inc. Firstly, 1.0 mg 525 nm QDs-MIP were dropped into 10 ml carbofuran aqueous solution with different concentrations and oscillated for 90 min. Secondly, the mixed solution was analyzed by the Cytoflex flow cyclometer using the 525/20 nm fluorescence channel for detection. Then, 10000 events were recorded at a medium flow rate for all measurements.

Results and Discussion

Characterization studies of QDs-MIP and QDs-NIP

The surface morphology of QDs-MIP and QDs-NIP was displayed by SEM. As shown in Fig. 2, the surface of PS seeds was smooth, while the surface of QDs-MIP and QDs-NIP was porous. Furthermore, the diameter of PS seeds was in the range of 2 - 3 μm , and the diameter of QDs-MIP and QDs-NIP was in the range of 8 - 10 μm , which indicated that the shells for QDs-MIP and QDs-NIP were successfully formed onto the surface of PS seeds. Meanwhile, it was found that QDs-MIP had a uniform spherical structure, excellent dispersibility and fluorescence property, which exactly met the requirements of flow cytometer analysis.

The energy spectrum diagram of QDs-MIP is shown in Fig. 2d. Cd, Se, Zn and S elements were detected by energy disperse spectroscopy. The S element could be partly brought into the QDs-MIP from SDS, and Cd, Se and Zn elements were all from CdSe/ZnS QDs. As expected, the QDs successfully attached to the surface of the MIPs.

FTIR spectroscopy was used to further characterize QDs-MIP

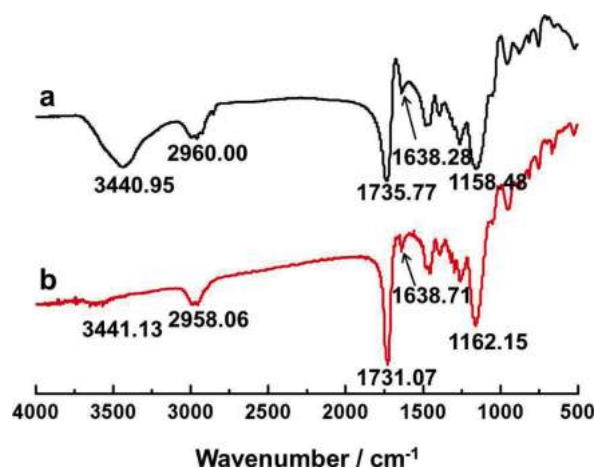


Fig. 3 FTIR spectra of (a) QDs-MIP and (b) QDs-NIP.

and QDs-NIP. The FTIR spectra of the QDs-MIP and QDs-NIP particles were recorded within the range of 500 - 4000 cm⁻¹ (Fig. 3). Not surprisingly, their major bands were in similar locations because the composition of QDs-MIP and QDs-NIP were similar. As shown in Fig. 3, the strong broad bands at 3440 and 3441 cm⁻¹ were the stretching vibrations of -OH, the 3440 and 3441 cm⁻¹ were the stretching vibrations of -CH₃ or -CH₂, and the 1158 and 1162 cm⁻¹ were the stretching vibrations of asymmetrical ester. The strong peaks at 1731 and 1735 cm⁻¹ were the stretching vibrations of C=O, which indicated that the crosslinkers (EGDMA) were successfully incorporated into the imprinted polymers. In addition, the weak peaks at 1638.28 and 1638.71 cm⁻¹ were the stretching vibrations of C=C, indicating that most of the functional monomer (MAA) and the crosslinkers (EGDMA) had the cross-linking reaction.³² Consequently, the results suggested that the MIPs and NIPs were successfully synthesized.

An adsorption isotherm is a measure of the relationship between the equilibrium concentration of bound and free guest over a certain concentration range and could be easily generated from equilibrium batch rebinding studies. Adsorption isotherm curves include Langmuir, Freundlich and Langmuir-Freundlich (F-L) isotherms, but the accuracy of Langmuir and Freundlich

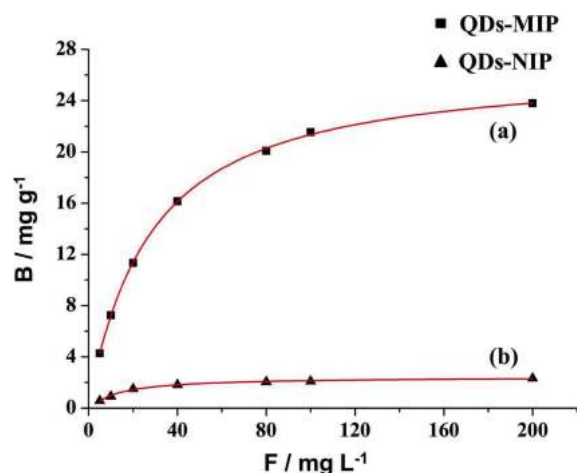


Fig. 4 Plots of the adsorption isotherms for QDs-MIP (a) and QDs-NIP (b).

Table 1 Langmuir-Freundlich fitting parameters for QDs-MIPs and QDs-NIPs

	$N_t/\text{mg g}^{-1}$	$a/\text{mg L}^{-1}$	m	R^2
QDs-MIPs	25.94	0.041	0.95	0.985
QDs-NIPs	2.60	0.12	0.77	0.993

curve fitting are not as good as L-F adsorption curve.³³ Therefore, L-F adsorption curve was chosen to analyze the data in this study. The formula is as follows:

$$B = \frac{N_t a F^m}{1 + a F^m} \quad (1)$$

where B is the concentration of bound, F is the concentration of free guest, N_t is the total of binding sites, m is the heterogeneity index, and a is related to the medium affinity constant.

The experimental adsorption isotherms were fitted to determine the heterogeneity. It was found that the experimental values were well represented by the Langmuir-Freundlich model (Fig. 4). The fitting parameters (Table 1) indicated QDs-MIPs had a much higher adsorption ($N_t = 25.94$) than QDs-NIPs ($N_t = 2.60$). The maximum adsorption capacity of MIPs was 10 times of the maximum adsorption capacity of NIPs. The specificity coefficient of carbofuran MIPs indicated that the carbofuran MIPs had one kind of site binding when adsorbing carbofuran and NIPs had multiple kinds of sites adsorption but does not form a specific binding site for carbofuran.

In the current study, carbofuran (template molecule) was entrapped in the polymer matrixes through hydrogen bond.³⁴ To further elucidate the high selectivity of QDs-MIP in aqueous media, QDs-NIP was prepared using the same method as those used for QDs-MIP without the template. Thus, the NIPs had the similar size distribution and morphological features. As shown in Fig. 5, the fluorescence intensity of QDs-NIP was 3.94 and 1.04 times of that of QDs-MIP before and after the adding of carbofuran. It can be seen that the fluorescence intensity of QDs-MIP decreased after the fluorescence quenching with carbofuran. In addition, the fluorescence intensity was restored almost to that of QDs-NIP, indicating that carbofuran were not completely removed from the recognition cavities in QDs-MIP. It was found that the QDs-MIP with fast adsorption and

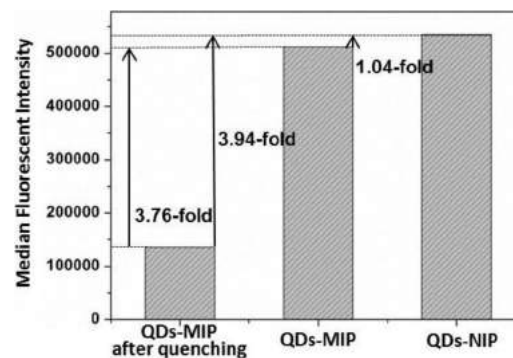


Fig. 5 Fluorescence intensity of QDs-MIP before and after fluorescence quenching with carbofuran and QDs-NIP.

desorption kinetics were actually suitable for the simple and rapid determination of analytes in aqueous media.

Fluorescence quenching analysis

As a sensing material for highly selective and sensitive optosensing of carbofuran, the design of our QDs-MIP composites is based on the fluorescence quenching in the presence of carbofuran. Nowadays there are various mechanism explanations, such as fluorescence resonance energy transfer, charge transfer and quantum dot surface lattice defects.^{30,35,36} In this work, ultraviolet spectrophotometer was employed to explore the mechanism of the fluorescence quenching. The UV-vis spectra of carbofuran and QDs-MIP are shown in Fig. S2 (Supporting Information). It was observed that the UV absorption of carbofuran was close to the band gap of QDs-MIP. It was known that the QDs-MIP valence band is full of charges. With a beam of light shining, the charges in the conduction bands of QDs-MIP will be transferred to the lowest unoccupied molecular orbital of the UV band of carbofuran. However, the charges cannot go back to the valence band, and results in fluorescence quenching. Moreover, there is no spectral overlap between the emission spectrum of QDs-MIP and the adsorption spectrum of the carbofuran, further suggesting that the mechanism of fluorescence quenching between carbofuran and QDs-MIP may be charge transfer.³⁶

Optosensing of carbofuran by QDs-MIP

Typical fluorescence quenching of QDs-MIP from 1 to 20 $\mu\text{g L}^{-1}$ was investigated. It was clearly observed that the QDs-MIP material, as a fluorescent probe, showed obvious fluorescence responses to the different concentrations of carbofuran, which was suitable for the practical application. In this system, the behavior of fluorescence quenching can be described by the Stern-Volmer equation.³⁷

$$F_0/F = 1 + K_{SV}[\text{CBF}] \quad (2)$$

where F_0 and F are the fluorescence intensities of QDs-MIP in the absence and presence of carbofuran, respectively. K_{SV} is the Stern-Volmer quenching constant, and $[\text{CBF}]$ is the carbofuran concentration. The equation can be used to quantify the K_{SV} value, and the ratio of QDs-MIP and QDs-NIP K_{SV} values ($K_{SV, \text{QDs-MIP}}/K_{SV, \text{QDs-NIP}}$) is defined as the imprinting factor (IF) which can further evaluate the selectivity of the sensing materials.

In this system, the quenching materials QDs-MIP with carbofuran satisfied the following equation: $F_0/F = 1.0029 + 0.06736[\text{CBF}]$, the correlation coefficient was 0.9968. The linear

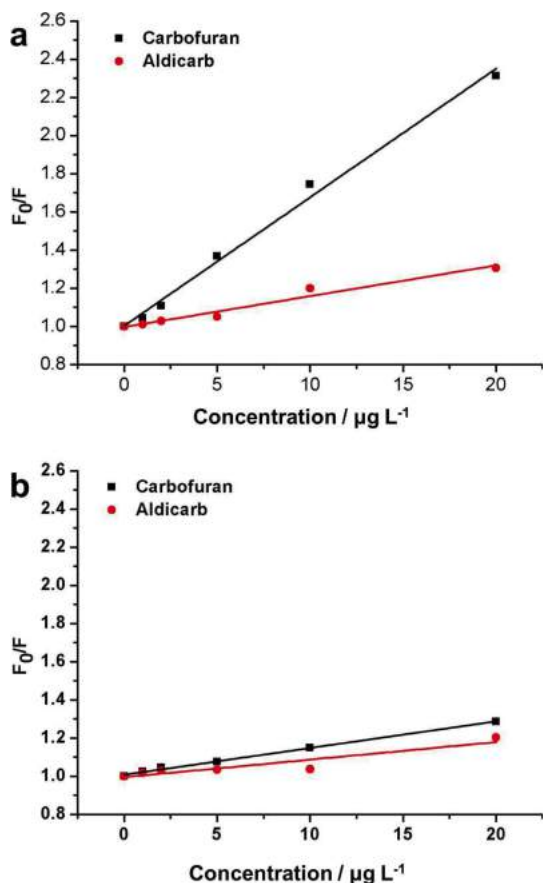


Fig. 6 Selectivity of (a) QDs-MIP and (b) QDs-NIP for carbofuran and aldicarb.

range of the calibration curve was over 1 – 20 $\mu\text{g L}^{-1}$ with a detection limit³⁷ of 0.2 $\mu\text{g L}^{-1}$. The quenching constant of QDs-MIP and QDs-NIP with addition of the indicated concentrations of carbofuran and aldicarb is shown in Fig. 6. The ratio of $K_{\text{SV,QDs-MIP}}$ and $K_{\text{SV,QDs-NIP}}$ is defined as the imprinting factor (IF) to evaluate the selectivity of the sensing materials. As expected, the $K_{\text{SV,QDs-MIP}}$ was much higher than those of analogue aldicarb, and the IF value was highest for carbofuran at 4.83. The obtained results illustrated that QDs-MIP in this experiment possessed high selectivity and specificity. Furthermore, the average detecting time of every sample was about 1 min, which was faster than the traditional analytical methods.

Selective adsorption on MIP based on QDs

The tailor-made recognition sites of the QDs-MIP composites that can selectively bound carbofuran. To further demonstrate the selectivity of QDs-MIP, aldicarb as structural analogue was involved. The relationships obtained for carbofuran and analogue interacting with QDs-MIP and QDs-NIP is shown in Fig. 7. The most intense fluorescence response to carbofuran and a weak fluorescence quenched effect to its analogue were observed. Nevertheless, the changes of QDs-NIP were similar for carbofuran and aldicarb. This demonstrated that because of the different structure of aldicarb, they cannot be absorbed into the customized recognition cavities formed in QDs-MIP. Meanwhile, there were no tailor-made recognition sites in QDs-NIP, so there was no obvious difference on the binding capacity of carbofuran and aldicarb.

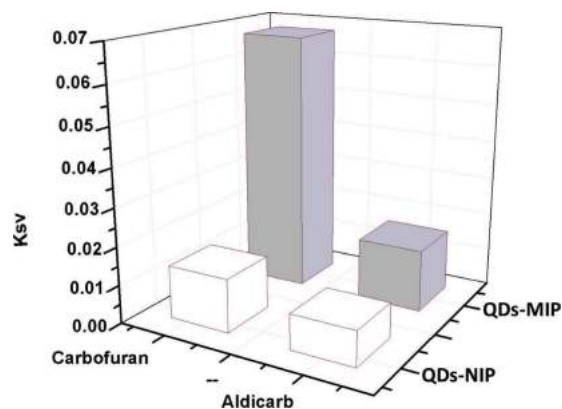


Fig. 7 Quenching constant of QDs-MIP and QDs-NIP with addition of the indicated concentrations of carbofuran and aldicarb.

Table 2 Spiked recovery results for the optosensing of CBF in water samples

Sample	Spiked level/ $\mu\text{g L}^{-1}$	Found/ $\mu\text{g L}^{-1}$ (means; $n = 3$)	Recovery, % ($n = 3$)
Tap water	2	1.97 ± 0.09	98.4 ± 4.5
	5	4.81 ± 0.22	96.2 ± 4.4
	10	9.41 ± 0.37	94.1 ± 3.7

Application to real sample analysis

In order to evaluate the feasibility of this method, the tap water samples collected from Shenyang (China) were analyzed. After the water samples were collected and filtered, the determination was carried out with the calibration curve method. Firstly, there was no response corresponding to carbofuran is observed in these tap water samples. Then, different concentrations of carbofuran (2, 5 and 10 $\mu\text{g L}^{-1}$) were added into these water samples. The experiment results are shown in Table 2. The recoveries of carbofuran in tap water samples were 94.1 ± 3.7 to $98.4 \pm 4.5\%$, indicating that QDs-MIP provide accurate measures of carbofuran in unknown water samples. Some analytical methods for carbofuran detection are summarized in Table S1 (Supporting Information). The recovery, precision and limit of detection (LOD) of the proposed method were comparable to other methods.^{1,2,4,5,38-42} In comparison with those methods, this method had the advantages of low cost, less toxic and fast analysis speed.

Conclusions

In this work, a facile strategy for the specific recognition and fluorescent determination of carbofuran was proposed based on the fluorescence quenching of QDs-MIP. By using the QDs-MIP as sample carriers of flow cytometry, the potential advantages of the method including high selectivity, high sensitivity and high throughput will further expand the development space of cytometric bead array and QDs-MIP sensing material in the near future. Although the method is still in its infancy, its low-cost, simple preparation and fast analysis speed all make this method attractive. A follow-up study will focus on optimizing and improving the performance of the procedure.

Acknowledgements

We gratefully appreciate financial support from the National Key Basic Research Development Project Program (16YFD0401201) and the Science and Technology Project Foundation of Shenyang (F16-107-4-00 and F15-177-6-00). The authors wish to express their gratitude to the anonymous reviewers for the stimulating suggestions and discussions.

Supporting Information

The SEM image of oil-soluble CdSe/ZnS quantum dots, UV-vis spectra of carbofuran and QDs-MIP, the relationship between fluorescent intensity and carbofuran concentration and the comparison of this method with other methods used in the literature are shown in the Supporting Information. This material is available free of charge on the Web at <http://www.jsac.or.jp/analsci/>.

References

- X. Sun, Y. Zhu, and X. Wang, *Food Control.*, **2012**, *28*, 184.
- A. Samphao, P. Suebsano, Y. Wonga, B. Pekec, J. Jitchareon, and K. Kalcher, *Int. J. Electrochem. Sci.*, **2013**, *8*, 3254.
- M. Younes and H. Galal-Gorchev, *Food Chem. Toxicol.*, **2000**, *38*, 87.
- "Guidelines for Drinking-Water Quality", 4th ed., **2011**, World Health Organization, Switzerland, 328.
- J. Wu, Q. Hong, Y. Chen, and S. Li, *Spectrosc. Spectral Anal.*, **2006**, *26*, 1716.
- P. Arnnok, N. Patdhanagul, and R. Burakham, *Chromatographia*, **2015**, *78*, 1327.
- S. Peng, J. Xiao, J. Cheng, M. Zhang, X. Li, and M. Cheng, *Microchim. Acta*, **2012**, *179*, 193.
- J. P. Dos Anjos and J. B. De Andrade, *Microchem. J.*, **2015**, *120*, 69.
- X. Ren, H. Liu, and L. Chen, *Microchim. Acta*, **2015**, *182*, 193.
- G. Raquel, J. C. Maria, and M. C. F. Ana, *Am. J. Anal. Chem.*, **2011**, *2*, 16.
- E. Takano, F. Tanaka, T. Ooya, and T. Takeuchi, *Anal. Sci.*, **2012**, *28*, 457.
- T. Kubo, K. Hosoya, and K. Otsuka, *Anal. Sci.*, **2014**, *30*, 97.
- W. Cheong, S. Yang, and F. Ali, *J. Sep. Sci.*, **2013**, *36*, 609.
- G. Guan, R. Liu, Q. Mei, and Z. Zhang, *Chem.—Eur. J.*, **2012**, *18*, 4692.
- H. Wei, G. Wang, H. Wu, Y. Luo, D. Li, and Q. Meng, *Acta Physico-Chemical Sin.*, **2016**, *32*, 201.
- A. Reisch and A. S. Klymchenko, *Small*, **2016**, *12*, 1968.
- C. Zhang, H. Cui, J. Cai, Y. Duan, and Y. Liu, *J. Agric. Food Chem.*, **2015**, *63*, 4966.
- D. Vasudevan, R. R. Gaddam, A. Trinchi, and I. Cole, *J. Alloys Compd.*, **2015**, *636*, 395.
- N. Samadi and S. Narimani, *Spectrochim. Acta, Part A*, **2016**, *163*, 8.
- H. M. Al-Saidi and M. S. El-Shahawi, *Spectrochim. Acta, Part A*, **2015**, *138*, 736.
- E. Luan, Z. Zheng, X. Li, H. Gu, and S. Liu, *Anal. Chim. Acta*, **2016**, *916*, 77.
- G. Fang, C. Fan, H. Liu, M. Pan, H. Zhu, and S. Wang, *RSC Adv.*, **2014**, *4*, 2764.
- X. Wei, Z. Zhou, T. Hao, Y. Xu, H. Li, K. Lu, J. Dai, X. Zheng, L. Gao, and J. Wang, *Microchim. Acta*, **2015**, *182*, 1527.
- X. Ren and L. Chen, *Biosens. Bioelectron.*, **2015**, *64*, 182.
- C. Xiao, Q. Liu, X. Dou, M. Yang, W. Kong, and L. Wan, *Chin. J. Anal. Chem.*, **2016**, *44*, 625.
- W. Ren, H. Liu, W. Yang, Y. Fan, L. Yang, Y. Wang, C. Liu, and Z. Li, *Biosens. Bioelectron.*, **2013**, *49*, 380.
- C. Xiao, W. Kong, Q. Liu, M. Yang, and L. Wan, *China Journal of Chinese Meteria Medica*, **2015**, *40*, 3515.
- J. Haginaka and H. Sanbe, *J. Chromatogr. A*, **2001**, *913*, 141.
- H. Sambea, K. Hoshina, R. Moaddel, I. W. Wainer, and J. Haginaka, *J. Chromatogr. A*, **2006**, *1134*, 88.
- Y. Zhao, Y. Ma, H. Li, and L. Wang, *Anal. Chem.*, **2012**, *84*, 386.
- Q. Zhang, Y. Han, W. Wang, L. Zhang, and J. Chang, *Eur. Polym. J.*, **2009**, *45*, 550.
- O. Y. F. Henry, D. C. Cullen, and S. A. Piletsky, *Anal. Bioanal. Chem.*, **2005**, *382*, 947.
- R. Umpleby, S. Baxter, Y. Chen, R. Shah, and K. Shimizu, *Anal. Chem.*, **2001**, *73*, 4584.
- Z. Xu, J. Wan, S. Liang, and X. Cao, *Biochem. Eng. J.*, **2008**, *41*, 280.
- R. Tu, B. Liu, Z. Wang, D. Gao, F. Wang, Q. Fang, and Z. Zhang, *Anal. Chem.*, **2008**, *80*, 3458.
- H. Wang, Y. He, T. Ji, and X. Yan, *Anal. Chem.*, **2009**, *81*, 1615.
- H. Liu, G. Fang, H. Zhu, C. Li, C. Liu, and S. Wang, *Biosens. Bioelectron.*, **2013**, *47*, 127.
- V. D. S. Salvatierra-Stamp, S. G. Ceballos-Magana, J. Gonzalez, J. M. Jurado, and R. Muniz-Valencia, *Anal. Bioanal. Chem.*, **2015**, *407*, 4661.
- R. Prasad, N. Upadhyay, and V. Kumar, *Microchem. J.*, **2013**, *111*, 91.
- S. Li, G. Yin, X. Wu, C. Liu, and J. Luo, *Electrochim. Acta*, **2016**, *188*, 294.
- G. F. Grawe, T. R. De Oliveira, E. D. Narciso, S. K. Moccellini, A. J. Terezo, M. A. Soares, and M. Castiho, *Biosens. Bioelectron.*, **2015**, *63*, 407.
- C. Fernandez-Ramos, D. Satinsky, and P. Solich, *Talanta*, **2014**, *129*, 579.